STRESS ANALYSIS FOR SCLERAL BUCKLING OF THE EYE

by

Raed Aldhafeeri

B. S. in Mechanical Engineering

King Fahd University of Petroleum and Minerals, 2009

Submitted to the Graduate Faculty of

Swanson School of Engineering in partial fulfillment

of the requirements for the degree of

M. S. in Mechanical Engineering

University of Pittsburgh

2015

UNIVERSITY OF PITTSBURGH

SWANSON SCHOOL OF ENGINEERING

This thesis was presented

by

Raed Aldhafeeri

It was defended on

July 15, 2015

and approved by

Patrick Smolinski, PhD, Associate Professor

Mark C Miller, PhD, Associate Professor

Qing-Ming Wang PhD, Professor

Thesis Advisor: Patrick Smolinski, PhD, Associate Professor

STRESS ANALYSIS FOR SCLERAL BUCKLING OF THE EYE

Raed Aldhafeeri, M. S.

University of Pittsburgh, 2015

Scleral buckling is a process in which a buckle or band is wrapped around the eye and tightened and is used to treat different eye disorders. The procedure can result in induced myopia by increasing the axial length of the human eye. This study was performed to assess how the application of a scleral buckle of various widths and tightness on eyes with decreased corneal thicknesses affects stresses and strains in the tissue and the anterior-posterior dimension. For this purpose, an axisymmetric finite element model of the eye was created where the mechanical properties of the tissues are assumed to be linearly elastic, the humors as incompressible fluid and the buckle as rigid. The buckles were chosen to have widths of 3, 5 and 7 mm with constrictions of 0.5, 1 and 1.5 mm and the reduced thicknesses of the cornea that were considered are 0, 25 and 50%. The results showed that as the buckle width and tightness increase, the axial length change of the eye increases. The maximum stress is greater for a thinner buckle with greater tightness. Also, the change in corneal thickness has a minor effect on the axial length and maximum stress. For scleral buckle selection, increased buckle width and construction lead to an increase in myopia. Eyes which have thinner cornea due to disease or LASIK procedure for example are more susceptible to this myopic shift than eyes with a normal corneal thickness.

TABLE OF CONTENTS

LIST OF TABLES

LIST OF FIGURES

1.0 INTRODUCTION

The eye is a pressurized shell with a complex geometry having multiple tissue layers. In the treatment of some eye diseases, the response of the eye to different surgeries may be related to material properties and geometry of different structures of the eye. The finite element method (FEM) is a common computational tool that is used to analyze stresses and displacement in objects with complex shapes and material properties and the method has been widely used to study eye biomechanics in stimulating impact, refractive surgeries, accommodation and some factors in eye diseases.

Scleral buckling is a common surgery for treatment of the retinal detachment (RD) in which a silicon band is placed and tighten around the circumferential globe of the eye. This procedure is believed to cause myopia (nearsightedness) by increasing the axial length of the eye (Harris et. al 1987, Smiddy et. al 1989, Okada et. al 2000). It has been proposed that different axial length changes may be due to the amount of the tightness and geometry of the buckle (Okada et. al 2000, Harris et. al 1987). This study is to assess the effect of different scleral buckle widths, amount of the tightness and corneal thinning on the axial length of the eye using finite element analysis.

An overview of the anatomy of the eye and the mechanical properties of the cornea and sclera is presented. Descriptions of the previous finite element models of the eye are discussed in term of the geometries, material properties, loading and the main results of each study. In the

methods section the details of the model in terms of the geometry, materials properties of the included tissues and boundary conditions with loading steps are presented. Results Of the modeling are given in terms of pressure change, axial length change and maximum stress as function of the scleral buckle width, tightness and thinning of the cornea.

2.0 BACKGROUND

2.1 ANATOMY OF THE EYE

Before discussing models of the eye, the anatomy of the eye will be introduced. The eye is held within fatty tissues in the skull and controlled by muscles. The shape of the eye is partial sphere (Figure 2.1) with two chambers that contain the aqueous and vitreous humors. The aqueous humor is water like and the vitreous has a jelly like consistency. Both fluids are responsible for maintaining the intraocular pressure (IOP) in the eye. The optic nerve head (ONH) inserts into the vitreous chamber wall at the back of the eye and the wall has of three layers of tissue: sclera, choroid and retina. The sclera is the white tissue and it is thicker than choroid and retina having a thickness of approximately 0.5-1 mm (Norman et. al 2011). The retina is the inner layer of the eye where the light is captured and is converted to signals transmitted to the brain through optic nerve. The lens serves to focus the light on the retina and it is attached to the sclera by zonular fibers from the ciliary body.

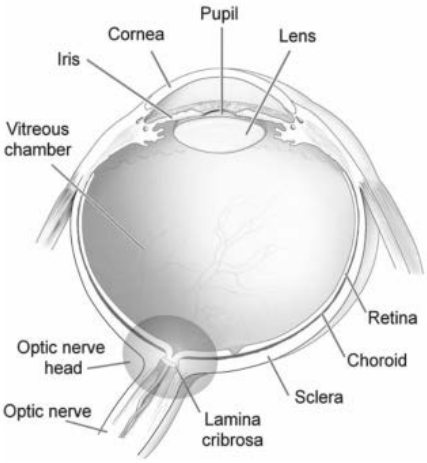

Figure 2.1: Cross section of the eye indicating different tissue structures (Sigal et. al 2009).

2.2 MECHANICAL PROPRTIES OF THE EYE TISSUE

Biological tissues are generally viscoelastic, anisotropic materials having a nonlinear stress-strain relationship (Bischoff et. al 2004). Of the tissues in the eye, the mechanical behaviors have been primarily investigated for sclera and cornea due to their significant involvement in surgeries and their structure importance.

Most of the mechanical testing of the sclera tissue has been conducted at low strain rates and nonlinearity has been always observed in the results. Woo et. al (1972) pressurized both hemispheres of the eye, and using simple finite element models, the elastic modulus of the sclera and cornea were estimated to be tri-linear functions. On the other hand, Friberg et. al (1998) and Graebel et. al (1977) represented the uniaxial stress-strain relationship results of the scleral tissue as linear and exponential, respectively. Moreover, the sclera stiffness and anisotropy have been examined in different locations within the eye. Battaglioli and Kamm (1982) concluded from compression testing that the radial compressive modulus of the sclera is less than the

circumferential modulus by two orders of magnitude. Through biaxial testing of posterior scleral tissue, Eilaghi et. al (2010) using a Fung exponential model, found that there were no significant difference in properties between nasal, temporal, superior and interior directions. Elsheikh et. al (2010a) approximated the stress-strain relation for anterior, equatorial and posterior scleral tissue with exponential relationships for low and high strain rates and concluded that the stiffness increased away from optic nerve head.

The mechanical properties of the corneal tissue have been also investigated experimentally. Andreassen et. al (1980) found that the keratoconus cornea is less stiffer than the normal cornea using uniaxial testing. The uniaxial tests of both Hoeltzel et. al (1992) and Wollensak et. al (2003) have confirmed the exponential nonlinearity of the stress-strain behavior of the cornea. Elsheikh et. al (2007) measured the Young's modulus of the cornea as a function of the age and intraocular pressure based on inflation testing. Recently, Petsche et. al (2012) have done experiments to measure the transverse shear modulus of the cornea. They found that the shear modulus is less than the tangent modulus by 2-3 orders of magnitude.

It can be noted that the mechanical properties of the tissues measured from the experiments varies among tests. One reason is that the temperature, age and hydration conditions of the samples before and during the tests were different and other factors are the initial stress in the sample and type of the mechanical loading that was applied.

3.0 FINITE ELEMENT STUDIES OF THE EYE

Different finite element models of the whole or portion of eye have been developed with different loading conditions to stimulate surgery or to examine other factors. Some of the models have been used for assessing stresses and deformation caused by medical procedures on different structures of the eye. In refractive surgeries, the curvature of the cornea is altered to correct nearsightedness and farsightedness, and finite element modeling has been used to predict the resultant curvature. Computer modeling has been also used to predict damage to the eye caused blunt force trauma. Finite element analysis was applied to evaluate optic nerve head surgery for the treatment of the eye diseases such as retinal venous drainage. Lens accommodation is another area where finite element simulation was used to study deformation of the lens curvature due to changes in the tension of the zonular fibers for increasing the optical power.

Bryant et. al (1987) used a two-dimensional model of the cornea with a uniform thickness and linear isotropic properties attached to a rigid portion of the sclera. Radial keratotomy (RK) surgery with 16 incisions (90% deep) caused inward and outward deflection at incisions and in the central cornea. In addition to having the same mode of the deformation as in in-vivo studies, a decrease in cornea power was closely matched to a reported value in the literature.

Hanna et. al (1989) created a shell model of the eye where the anisotropic cornea curvature was given by Lotmar's equation and the sclera curvature was approximated using the

projection of two different ellipses to account for varying thickness. When pressurized the results showed that the spherical stresses have the same magnitude at the limbus where the cornea and sclera curvature meet and a cornea incision has more effect on the peripheral corneal profile than a limbus incision.

Based on a simple fiber orientation in the stroma, Pinsky and Datye (1991) created the first finite element model for an anisotropic spherical cornea fixed at the limbus where different radial keratotomy incisions were applied to the cornea. Their results showed that increasing depth and optical zone diameter of the incision decreases the optical power with internal deflections and the results approximately matched in-vivo measurements.

Bryant and McDonnell (1996) have investigated four constitutive models using finite element model of an aspheric cornea, namely: linear elastic and isotropy, linear elastic with transverse isotropy, nonlinear elastic with isotropy and hyperelastic (Ogden's law). To investigate the effect of nonlinear strain measures, the linear elastic model was analyzed with linear and nonlinear strain measures. By comparing the results to experimental tests with an applied pressure of 40 mmHg, the nonlinear isotropic model had the best fit to the experimental data. Furthermore, the effect due to the geometric nonlinearity was less significant than the nonlinearity in properties, and there was not a significant difference between isotropic and transverse isotropic model.

Uchio et. al (1999) have created a dynamic model that included more structures of the eye, such as the iris, choroid, lens, vitreous and aqueous humor, where the humors were modeled as solids and tissues as part of both sclera and cornea shell. They did experimental tests to determine the nonlinear stress-strain relationships, Poisson's ratios, and failure limit of the cornea and sclera. Because cornea and sclera were modeled as single body and the internal

tissues as another body, the contact between them was modeled as a frictional contact and the whole model was constrained at the optic nerve head. A nonlinear explicit finite element solver results identified the size and velocity of missiles that would cause the rupture of the cornea and sclera.

Bellezza et. al (2000) have created simple models of the eye with different geometries, sclera thicknesses and cross section areas of the optic nerve head (Figure 3.1). For optic nerve head, the material properties were linear and approximated relative to sclera. With an applied intraocular pressure, their results showed that increased radius of the eye will just increase the stress in sclera. However, models with a smaller sclera thickness and optic nerve head cup with elliptical shape will have larger stresses on posterior sclera.

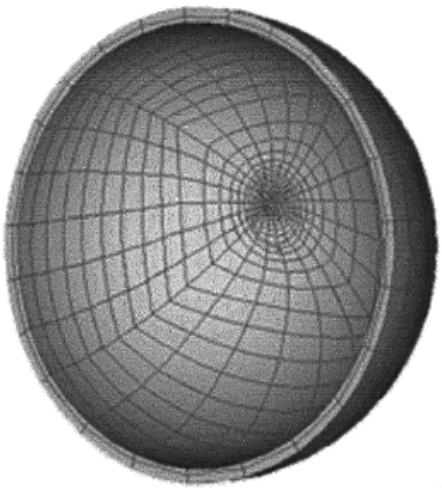

Figure 3.1: The posterior model of the sclera (Bellezza et. al 2000).

The VTEM model (Figure 3.2) is the more validated dynamic model generated in the impact biomechanics laboratory at Virginia Tech (Stitzel et. al 2002). The axisymmetric model

which is fixed at the optic nerve head involves more detailed geometry, and the humors were modeled using equation of state. Detailed properties of structures were implemented where nonlinear data of cornea and the sclera were extracted from the experiments done by Uchio et. al (1999) for their model. The dynamic model used experiments done in the same research work where human eyes were subjected to impact by different objects and recorded the displacement with high speed camera. The dynamic experimental and finite element displacement approximately matched at some values. Since then, VITEM model is still widely in used for blunt trauma with some modifications. Weaver et. al (2011) have used the model for simulating many experimental eye impact tests that exist in literature where different projectiles made of different materials were used such as: airsoft pellets, baseball, air gun pellets, paintball, foam, and rods. Liu et. al (2013) have included retina tissue in the model with adhesion criterion for modeling retinal detachment in blunt trauma. Rossi et. al (2011) have also used the same model where the sclera was modeled as linear elastic material and the other tissues with a linear equation of state for investigating the effects of the blunt trauma shockwave on the eye. The results showed that posterior retina has larger wave propagation which may cause macular and peripheral retinal injuries.

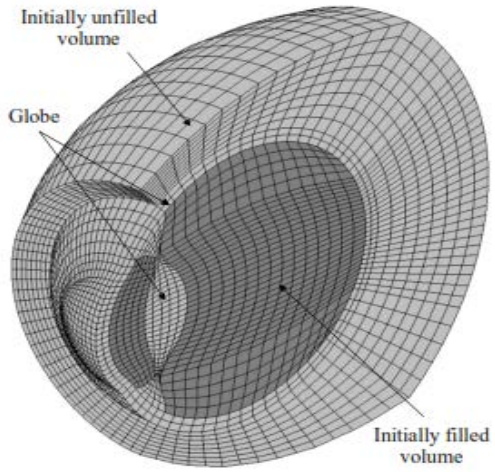

Figure 3.2: VTEM model (Stitzel et. al 2002).

Sigal et. al (2004) have created simple eye models fixed at the optic nerve, and included complex optic nerve head tissues with approximated properties relative to sclera where all of the tissue are assumed as linear elastic isotropic. Along with experimental tests, they clarified that optic cup shape (Figure 3.3) has a major effect on strain and stress level in different optic nerve head tissues. A three-dimensional version of this model was used again by the same research group for investigating the dominated mode of the strain within optic nerve head tissues as the intraocular pressure increase (Sigal et. al 2007). With an intraocular pressure increase up to 50 mmHg, they concluded that compressive strain is higher than shear and extension where higher compressive strain was in neural tissue.

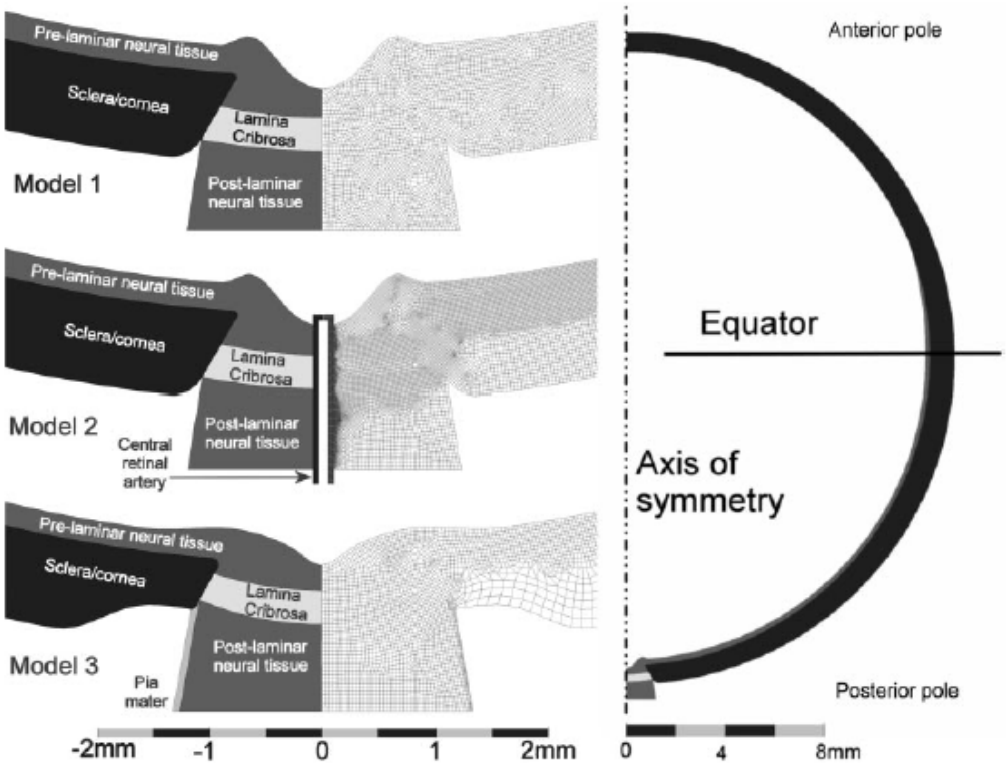

Figure 3.3: The three proposed geometries of the nerve cup and the eye model (Sigal et. al 2004).

Liu et. al (2006) created two models of the detailed geometry of composite lenses radially fixed and attached to three zonular fibers (Figure 3.4). All the model parts were assumed to be linear elastic where the elastic constants of the composite lens layers were extracted from previous experimental tests and the properties for zonular fibers were approximated. The first model indicated that an increase in intraocular pressure and movement of ciliary body will cause thinning of the lens which changes its optical power. The other model demonstrated the mechanism of accommodation where the lens becomes thicker because of relaxed anterior and posterior lens and extension of equatorial fiber.

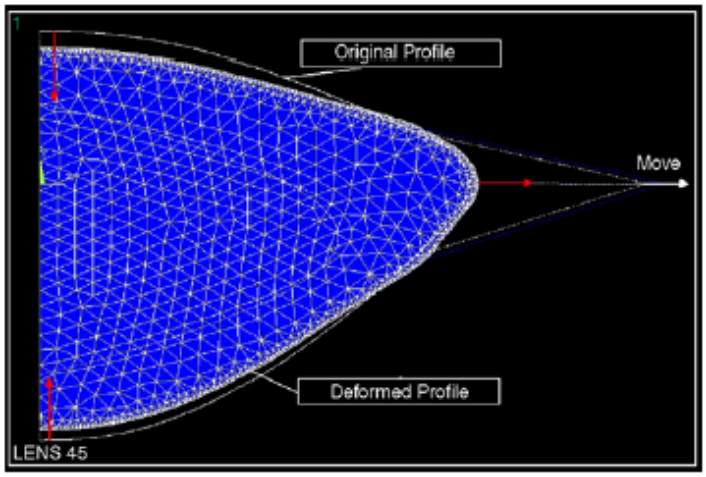

Figure 3.4: Original and deformed profile of the lens under displacement of the fibers (Liu et. al 2006).

Friberg et. al (2008) investigated the effects of radial optic neurotomy (RON) on retina vein within optic nerve head. Three-dimensional linear elastic hemispherical model was created for this purpose. With constant intraocular pressure inside the model and different pressure levels up to 75 mmHg in the vein, the model showed that the vein diameter was not significantly affected by the surgical procedure.

To study cornea refractive correction, Roy and Dupps (2009) have created an axisymmetric eye model with most of the eye structures to account for the limbus and lens movement during elevated intraocular pressure. The model all structures with isotropic linear elastic materials except for the cornea and the LASIK wound. They used weak and stiff properties reported in literature for the cornea linear hyperplastic model. For studying the effect of the boundary conditions, they used a simple model of the cornea fixed at the limbus and a whole eye model constrained at the optic nerve. The results showed that by increasing the intraocular pressure up to 30 mmHg for different cornea cut thicknesses, the displacement of the

cornea curve had a significant difference between the fixed cornea and the whole eye model. Moreover, the anterior chamber depth was decreasing for the stiff cornea but increasing for the weak cornea.

In the summary the finite element method has been widely used for simulating eye biomechanics under different loadings or surgical treatments. The finite element method can give insight into the mechanical response under these different conditions. The models varied according to the tissue constitutive models used and the structures of that were modelled.

4.0 METHODS

In this section the methods for modeling the effect of the sclera buckling on the eye with a normal and thin cornea using finite element software (ANSYS 16.0) will be discussed. Using a two-dimensional axisymmetric model of the eye, the eye structures included in this study with their geometries will be illustrated. The constitutive models and constants are defined along with the boundary conditions and loading steps.

4.1 EYE STRUCTURES

The eye axial diameter and the thickness of anterior, equatorial and posterior sclera (Figure 4.1) were taken to be average values measured by Norman et. al (2010) of 23.78, 0.8, 0.5 and 1 mm, respectively. The cornea profile was created using Lotmar's Equation (Lotmar 1971):

$$y = \frac{x^2}{r_0}\left[1 + a\left(\frac{x}{r_0}\right)^2 + b\left(\frac{x}{r_0}\right)^4\right]$$

where y describes the profile of the cornea along the geometrical axis as a function of its height x from the axis, r_0 is the radius of central curvature of the cornea and a and b are coefficients equal to 5/28 and 1/12, respectively. The cornea diameter was 11.7 mm and its thickness at

center is 0.587 mm. The anterior and posterior curvature radii are 7.8 and 6.6 mm, respectively (Hanna et. Al 1989).

The lens anterior and posterior curvatures can be also generated using equations (Fincham's profile) given by (Chien et. al 2003):

$$y_a(\theta) = (1.385901742692342 - 0.2185006863066996 + 0.045295982599325 57\theta^4)cos\theta$$

$$y_p(\theta) = (2.419123934364831 - 0.484144752446502 - 0.016755183522995 85\theta^4)cos\theta$$

$$r = 4.3\ sin\theta \qquad \text{all in mm}$$

where y_a, y_p define the anterior and posterior lens curvatures along the geometrical axis, respectively, and r is the radius of each curvature. θ is the angle between the coincide point of both curvatures and the geometrical axis where it is $0 \leq \theta \leq \pi/2$ for an axisymmetric lens.

The retina was assumed to have a constant thickness of 0.2 mm (Liu et. al 2013). The dimensions of ciliary body and zonouls fibers were estimated to their in vivo shapes and for connecting the cornesclera shell with the lens. The dimensions of the eye are shown in Figure 4.1.

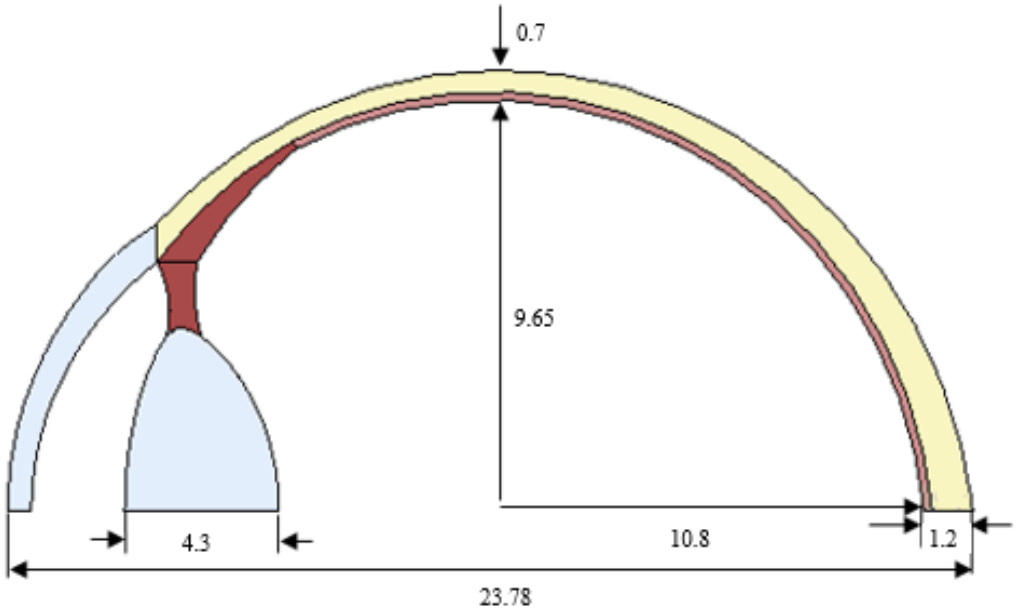

Figure 4.1: Dimensions of eye structures (mm).

4.2 TISSUE MATERIAL PROPRTIES

In previous models, most structures of the eye were considered as linearly elastic, isotropic materials. However, the constitutive model of the cornea and sclera have been modelled as linearly elastic and isotropic (Bryant et. al 1987, Bryant and McDonnell 1996, Bellezza et. al 2000, Sigal et. al 2004 and Friberg et. al 2008), linearly elastic with transverse isotropic (Hanna et. al 1989 and Bryant and McDonnell 1996) or as isotropic hyperelastic (Bryant and McDonnell 1996 and Uchio et. al 1999) materials.

For the linearly elastic, transversely isotropic model, the radial modulus was approximated relative to the in-plane modulus based on the Battaglioli and Kamm (1982) experiment and a shear modulus with Poisson ratio were based on assumptions. For all of the

material constants in the isotropic hyperelastic constitutive model to be defined, other types of experimental tests needed, for example, biaxial, shear and volumetric tests.

Due to a lack of full data on material constant, in this study, the cornea and sclera were taken to be isotropic linearly elastic materials. Similarly, the other tissue were taken to be linearly elastic. The values of the linear elastic properties for all tissues are given in Table 4.1. Due to their high content of water, the aqueous and vitreous humors were assumed to be incompressible fluids having same density as for water (1000 Kg/m^3).

Table 4.1: Mechanical properties of different eye tissues.

Tissue	E (MPa)	v	Reference
Sclera	3	0.47	Sigal et. al 2004, Uchio et. al 1999
Cornea	1.5	0.42	Rossi et. al 2011, Uchio et. al 1999
Retina	0.02	0.4999	Jones et. al 1992
Lens	6.88	0.4999	Czygan and Hartung 1996
Zonulus	0.35	0.4	Michael et. al 2012, Power et. al 2002
Ciliary Body	11	0.4	Power et. al 2002

4.3 BOUNDARY CONDTIONS AND LOADING

The finite element axisymmetric two-dimensional model of the eye is shown in Figure 4.2 for the cross section of the eye. Axisymmetric 6-node triangular elements are used for all solid tissues and aqueous and vitreous humors were represented by axisymmetric hydrostatic fluid elements. Since the buckle band is stiffer relative to the tissue, it is assumed to be a rigid material (Figure 4.3). A contact analysis is used between the sclera and the bands with zero friction coefficient.

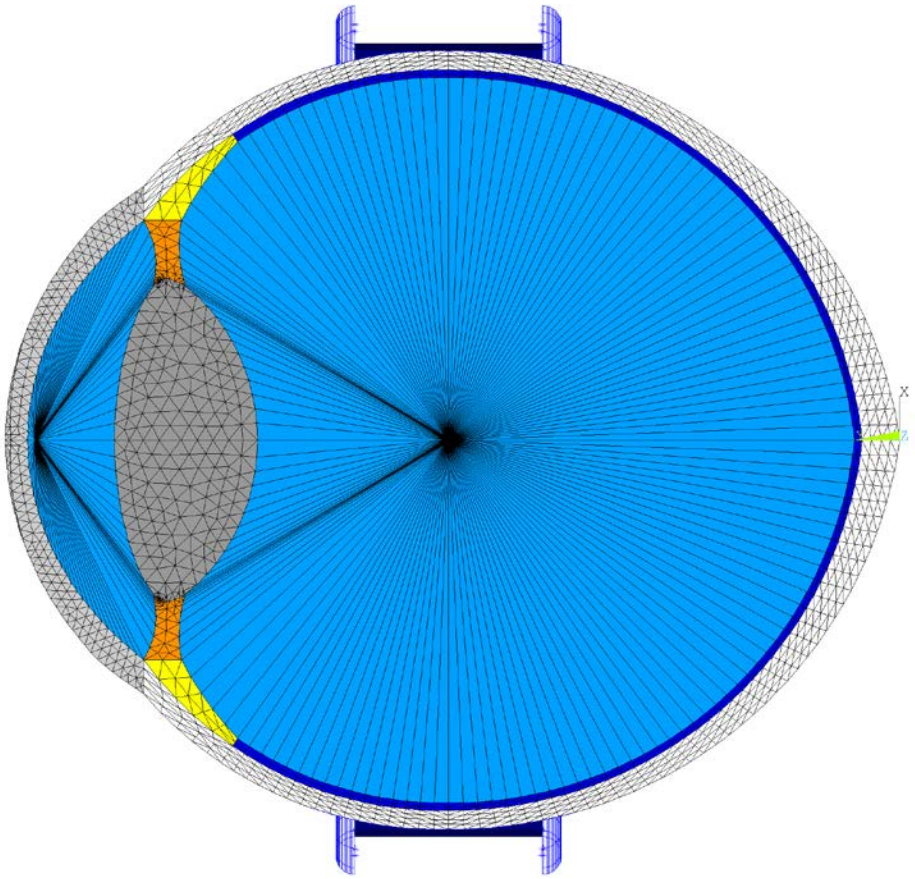

Figure 4.2: The finite element model of the eye and the buckle.

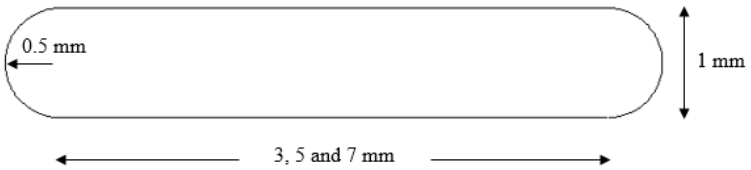

Figure 4.3: Cross-sectional geometry of the scleral buckle strip.

The axisymmetric model is constrained at the middle of equatorial sclera and along the axisymmetric axis. The main steps in applying loads are shown in Figure 4.4. To pressurize the model, an intraocular pressure of 2 kPa is applied in both humors. After pressurization, elements are removed from the cornea to consider reduced thickness cases. The reductions are 25% and 50% of the central cornea thickness with the same optical zone radius of 3 mm. At the final loading stage, the eyes are constricted by either a 3, 5 or 7 mm width band to include the effect of scleral buckling tightness. The constriction of the band that were considered were 0.5, 1 and 1.5 mm.

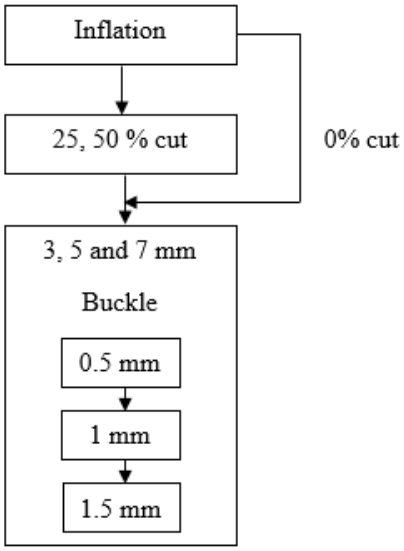

Figure 4.4: The main steps of the analysis.

5.0 RESULTS

The main items of interest in the results are the stress in the sclera and the change in the axial length of the eye. The stress in the sclera is relevant since it is the main structural element of the eye and the axial length of the eye has an effect on vision.

Before considering the specific results mentioned, some general results were considered to evaluate if the mechanics of the model had the behavior that was expected. When the thickness of the cornea was reduced on the pressurized eye, the curvature changed and displaced in the reduction region as shown in Figure 5.1. In addition to the change of the curvature, the reduction in thickness resulted in a less than 1.5% drop in the intraocular pressure in vitreous and aqueous humors. For the final step which is of major interest, the applied radial displacements of 0.5, 1, 1.5 mm to each band on the normal and reduced corneal thickness eye resulted in increases in the pressure of both chambers, the axial length of the eye and the concentrated stresses at the edges of the buckle. A sample result showing the stress distribution is given in Figure 5.2.

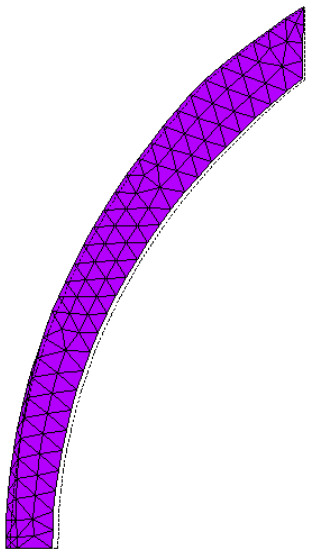

Figure 5.1: Deformation profile due to 25% reduction of the axisymmetric cornea.

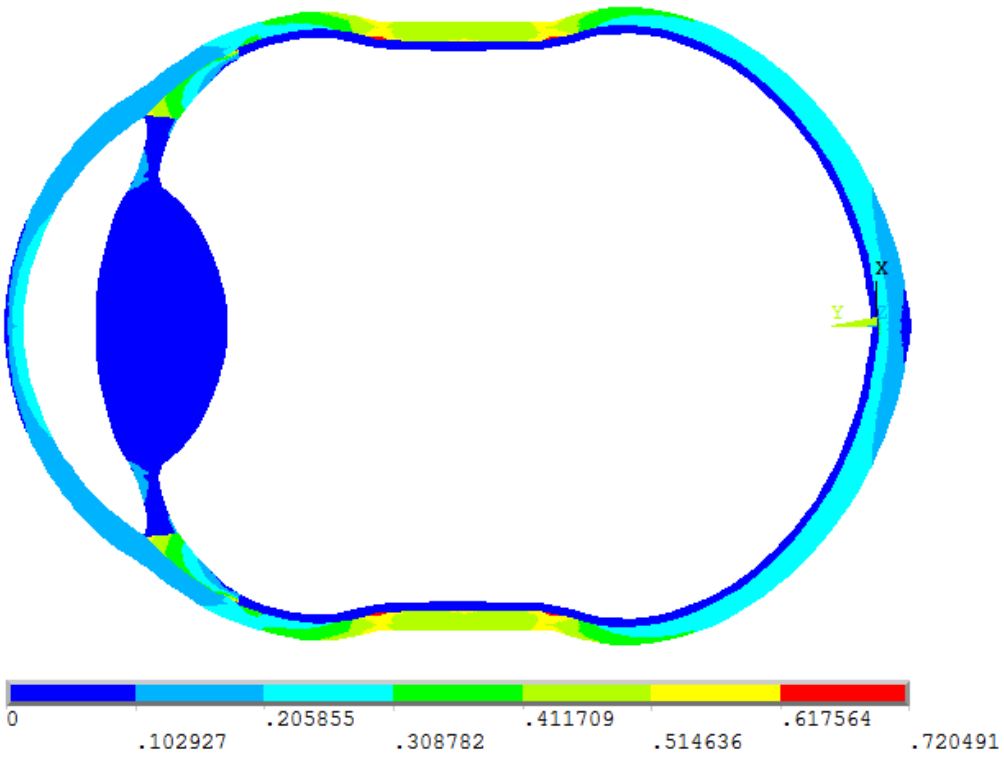

Figure 5.2: Von Mises stress (in MPa) and deformation profile for 25% cut, 5mm band with 1.5mm displacement model.

The numerical values of the pressure in each humor due to the displacements of the buckles are given in Table 5.1 for the standard thickness cornea eye model. It shows that the pressure increases as the tightness and buckle width increase especially in the vitreous humor since the vitreous chamber has more deformation than the aqueous chamber. It can be also noted that the pressure values are similar for all buckle widths with 0.5 mm constriction and this can be explained by the equality of the contact area at this small displacement between the buckle and the sclera.

Table 5.1: Pressure in the humors (kPa)

Buckle Width	3mm		5mm		7mm	
Displacement	vitreous	aqueous	vitreous	aqueous	vitreous	aqueous
0.5 mm	7.29	6.6	7.87	7.1	7.88	7.1
1 mm	16.46	14.14	20.19	17.09	22.22	18.67
1.5 mm	28.21	23.08	35.99	28.73	42.43	33.27

The initial axial length is taken to be the distance between the anterior of the retina and the anterior of the inflated normal or thinned cornea which is measured for 0, 25, and 50% thickness reductions as 23.84, 23.71 and 23.58 mm, respectively. The percent change of the axial length of the eye is given in Figure 5.3 as a function of buckle width, buckle construction and corneal thickness reduction. It shows that the percent change of the axial length increases as the buckle width and the amount of the tightness increases. In comparing the percent change between different cornea thicknesses, the differences are less than 1%.

The maximum scleral von Misses stress are given in Figure 5.4 as a function of buckle width, buckle construction and corneal thinning. In all cases, the maximum stress is located at the edges of the buckle is higher for the thin band and small tightness and it is almost same for each corneal thickness.

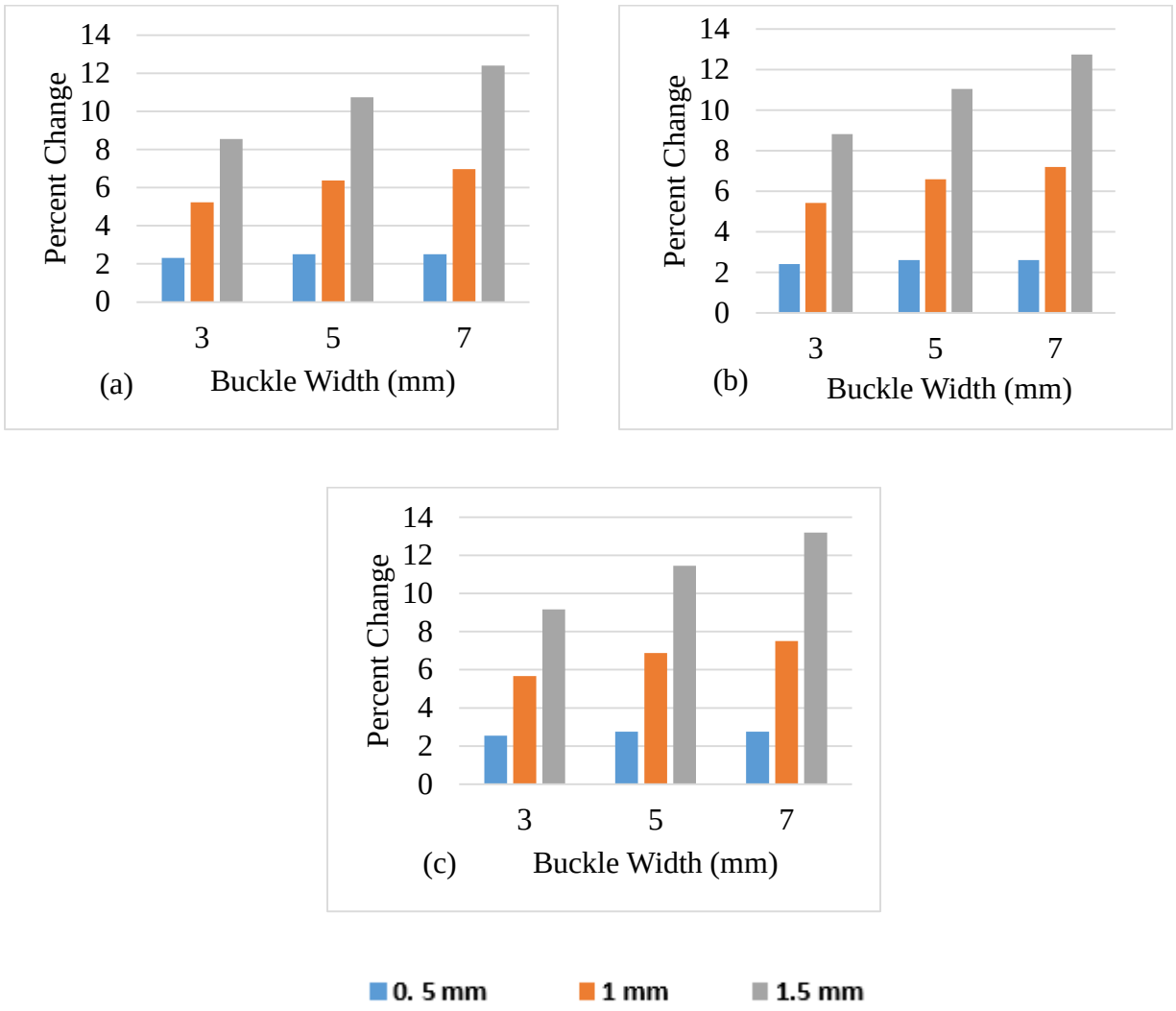

Figure 5.3: Percent change of the axial length as a function of buckle width, construction and corneal thickness reduction, (a) 0% reduction, (b) 25% reduction, (c) 50% reduction.

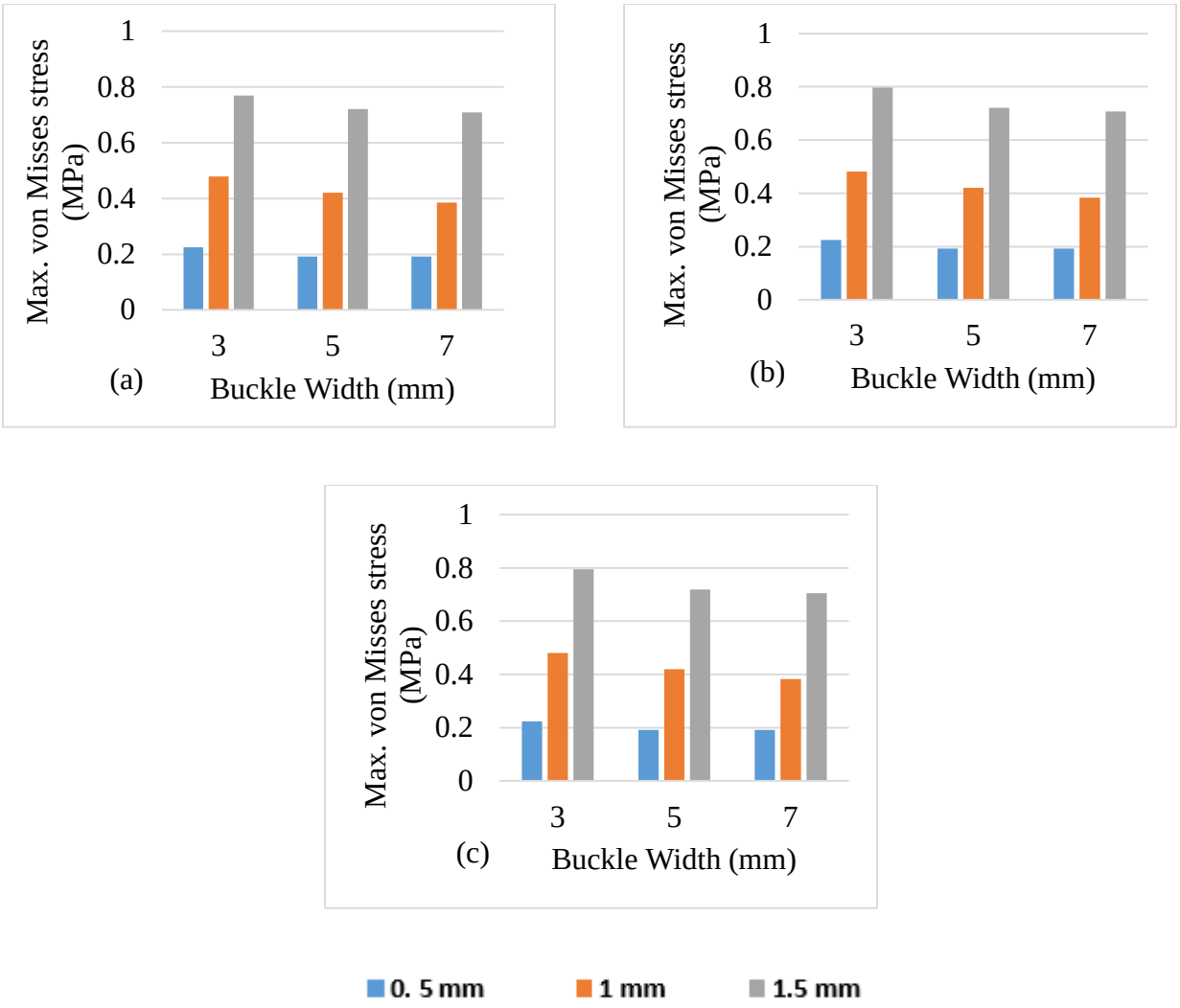

Figure 5.4: Maximum von Mises stress as a function of buckle width, construction and corneal thickness reduction, (a) 0% reduction, (b) 25% reduction, (c) 50% reduction.

To assess the effect of mesh refinement on the results, the number of elements in the sclera, which is the main structural tissue of the eye, was varied. This was done for the case of a 5 mm buckle width with a 1.5 mm constriction and for the cornea with a 25% reduction in thickness. For this the number of elements across its thickness was increased from 8 to 12

elements. Comparison of the results showed that the axial length change varied from 2.62 to 2.58 mm (1.65%) and the maximum von Mises stress increased from 721 to 750 kPa (4%). Based on this result, the model with 8 elements across the thickness of the sclera was deemed sufficient for the study.

6.0 CONCLUSIONS

The stress analysis for the scleral buckling of the eye was explored using finite element analysis and the effect of the scleral buckling selection and corneal thinning on the axial length of the eye was evaluated.

An axisymmetric finite element model of the human eye was constructed in terms of the known geometries and material properties. The eye structures included the sclera, cornea and lens.. The properties of the tissue were chosen to be linear elastic based on properties available in the literature and the humors were considered incompressible fluids. The scleral band was modeled as rigid. The effect of different band widths and constrictions and different corneal thickness on the axial length of the eye were evaluated.

Based on this model, the results showed that the axial length of the eye increases as the width of the buckle and the amount of the tightness increase and a thinner buckle with greater constriction will produce higher the maximum stress concentration at the edges than wider buckle. Cornea thinning shows less effect on the axial length and the maximum stress.

Because of the lack of the materials constants, one limitation of the model is the linear elastic properties used for the tissue. Experimental characterizations of the hyperelastic constants for the eye tissue especially for the sclera and cornea would be very advantageous in modeling the eye using finite element analysis.

BIBLIOGRAPHY

Andreassen, T. T., Simonsen, A. H., & Oxlund, H. (1980). Biomechanical properties of keratoconus and normal corneas. *Experimental Eye Research, 31*(4), 435–41.

Battaglioli, J. L., & Kamm, R. D. (1984). Measurements of the compressive properties of scleral tissue. *Investigative Ophthalmology and Visual Science, 25*(1), 59–65.

Bellezza, A., Hart, R., & Burgoyne, C. (2000). The optic nerve head as a biomechanical structure: initial finite element modeling. *Investigative Ophthalmology & Visual Science*, *41*(10), 2991–3000.

Bischoff, J. E., Arruda, E. M., & Grosh, K. (2004). A rheological network model for the continuum anisotropic and viscoelastic behavior of soft tissue. *Biomechanics and Modeling in Mechanobiology*, *3*(1), 56–65.

Bryant, M. R., Velinsky, S. A., Plesha, M. E., & Clarke, G. P. (1987). Computer-aided surgical design in refractive keratotomy. *The CLAO Journal : Official Publication of the Contact Lens Association of Ophthalmologists, Inc*, *13*(4), 238–42.

Bryant, M. R., McDonnell, P. J. (1996). Constitutive laws for biomechanical modeling of refractive surgery. *Journal of Biomechanical Engineering*, 118(4), 473-81.

Chien, C.H., Huang, T., Schachar, R.A., (2003). A mathematical expression for the human crystalline lens. *Comprehensive Therapy*, 29 (4), 245–258.

Czygan, G., Hartung, C. (1996). Mechanical testing of isolated senile human eye lens nuclei. *Medicine Engineering and Physics*, 18(5): 345-349.

Eilaghi, A., Flanagan, J. G., Tertinegg, I., Simmons, C. a, Wayne Brodland, G., & Ross Ethier, C. (2010). Biaxial mechanical testing of human sclera. *Journal of Biomechanics*, *43*(9), 1696–701.

Elsheikh, A., Wang, D., Pye D. (2007). Determination of the modulus of elasticity of the human cornea. *Journal of Refract Surgery*,23(8),808-18.

Elsheikh, A., Geraghty, B., Alhasso, D., Knappett, J., Campanelli, M., & Rama, P. (2010). Regional variation in the biomechanical properties of the human sclera. *Experimental Eye Research*, *90*(5), 624–33.

Friberg, T. R., & Lace, J. W. (1988). A comparison of the elastic properties of human choroid and sclera. *Experimental Eye Research*, *47*(3), 429–36.

Friberg, T. R., Smolinski, P., Hill, S., & Kurup, S. K. (2008). Biomechanical assessment of radial optic neurotomy. *Ophthalmology*, *115*(1), 174–80.

Graebel, W. P., & van Alphen, G. W. H. M. (1977a). The Elasticity of Sclera and Choroid of the Human Eye, and Its Implications on Scleral Rigidity and Accommodation. *Journal of Biomechanical Engineering*, *99*(4), 203–208.

Hannn, K. D., & Jouve, E. (1989). Computer Simulation of Arcuate and Radial Incisions Involving the Corneosc1eral Limbus. *Eye* 227–239.

Hoeltzel, D.A., Altman, P., Buzard, K., Choe, K., (1992). Strip extensiometry for comparison of the mechanical response of bovine, rabbit, and human corneas. *Journal of Biomechanical Engineering*,114 (2), 202–215.

Harris, M.J., Blumenkranz, M.S., Wittpenn, J., Levada, A., Brown, R., Frazier-Byrne, S., (1987). Geometric alterations produced by encircling scleral buckles: biometric and clinical consideration. *Retina*, 7:14–9.

Jones, I.L., Warner, M., Stevens, J.D., (1992). Mathematical modeling of the elastic properties of retina: a determination of Young's modulus. *Eye* (Lond) 6, 556–559.

Liu, X., Wang, L., Wang, C., Sun, G., Liu, S., & Fan, Y. (2013). Mechanism of traumatic retinal detachment in blunt impact: a finite element study. *Journal of Biomechanics*, *46*(7), 1321–7.

Liu, Z., Wang, B., Xu, X., & Wang, C. (2006). A study for accommodating the human crystalline lens by finite element simulation. *Computerized Medical Imaging and Graphics : The Official Journal of the Computerized Medical Imaging Society*, *30*(6-7), 371–6.

Lotmar W. (1971). Theoretical eye model with aspherics. *Journal Optical Society of America*, 61: 1522-9.

Norman, R. E., Flanagan, J. G., Sigal, I. a, Rausch, S. M. K., Tertinegg, I., & Ethier, C. R. (2011). Finite element modeling of the human sclera: influence on optic nerve head biomechanics and connections with glaucoma. *Experimental Eye Research*, *93*(1), 4–12.

Michael, R., Mikielewicz, M., Gordillo, C., Montenegro, G. a, Pinilla Cortés, L., & Barraquer, R. I. (2012). Elastic properties of human lens zonules as a function of age in presbyopes. *Investigative Ophthalmology & Visual Science*, *53*(10), 6109–14.

Okada, Y., Nakamura, S., Kubo, E., Oishi, N., Takahashi, Y., Akagi, Y. (2000). Analysis of Changes in Corneal Shape and Refraction Following Scleral Buckling Surgery. *Japan Journal of Ophthalmology*, 44, 132–138.

Petsche, S.J,, Chernyak, D., Martiz, J., Levenston, M.E., Pinsky, P.M. (2012). Depth-dependent transverse shear properties of the human corneal stroma. *Investigative Ophthalmology &Visual Science*, 53(2), 873-80.

Pinsky, P. M., & Datye, D. V. (1991). A microstructurally-based finite element model of the incised human cornea. *Journal of Biomechanics*, *24*(10), 907–22.

Power, E.D., Duma, S.M., Stitzel, J.D., Herring, I.P., West, R.L., Bass, C.R., Crowley, J.S., Brozoski, F.T., (2002). Computer modeling of airbag-induced ocular injury in pilots wearing night vision goggles. *Aviation, Space, and Environmental Medicine***,** 73, 1000–1006

Rossi, T., Boccassini, B., Esposito, L., Iossa, M., Ruggiero, A., Tamburrelli, C., & Bonora, N. (2011). The pathogenesis of retinal damage in blunt eye trauma: finite element modeling. *Investigative Ophthalmology & Visual Science*, *52*(7), 3994–4002.

Roy, A.S., Dupps, W.J. Jr. (2009). Effects of altered corneal stiffness on native and postoperative LASIK corneal biomechanical behavior: a whole-eye finite element analysis. *Journal of Refractive Surgery*, 25(10), 875-87.

Sigal, I. a, Flanagan, J. G., Tertinegg, I., & Ethier, C. R. (2004). Finite element modeling of optic nerve head biomechanics. *Investigative Ophthalmology & Visual Science*, *45*(12), 4378–87.

Sigal, I. a, Flanagan, J. G., Tertinegg, I., & Ethier, C. R. (2007). Predicted extension, compression and shearing of optic nerve head tissues. *Experimental Eye Research*, *85*(3), 312–22.

Sigal, I. a, Flanagan, J. G., Tertinegg, I., & Ethier, C. R. (2009). Modeling individual-specific human optic nerve head biomechanics. Part I: IOP-induced deformations and influence of geometry. *Biomechanics and Modeling in Mechanobiology*, *8*(2), 85–98.

Smiddy, W.E., Loupe, D.N., Michels, R.G., Enger, C., Glaser, B.M., deBustros, S. (1989). Refractive changes after scleral buckling surgery. *Archives of Ophthalmology*, 107(10):1469-71.

Stitzel, J. D., Duma, S. M., Cormier, J. M., & Herring, I. P. (2002). A Nonlinear Finite Element Model of the Eye with Experimental Validation for the Prediction of Globe Rupture, *46*(November).

Uchio, E., Ohno, S., Kudoh, J., Aoki, K., & Kisielewicz, L. T. (1999). Simulation model of an eyeball based on finite element analysis on a supercomputer. *British Journal of Ophthalmology*, *83*(10), 1106–1111.

Weaver, A. a, Kennedy, E. a, Duma, S. M., & Stitzel, J. D. (2011). Evaluation of different projectiles in matched experimental eye impact simulations. *Journal of Biomechanical Engineering*, *133*(3), 031002.

Wollensak, G., Spoerl, E., Seiler, T. (2003) Stress-Strain measurements of human and porcine corneas after riboflavin-ultraviolet-A-induced cross-linking. J. *Cataract Refractive Surgery*. 29(9), 1780-5.

Woo, S., Kobayashi, A., Schlegel, W. A., & Lawrence, C. (1972). Nonlinear material properties of intact cornea and sclera. *Experimental Eye Research*, *14*(1), 29–39.